

Proton-Assisted Hydrogen Activation on Polyhedral Cations

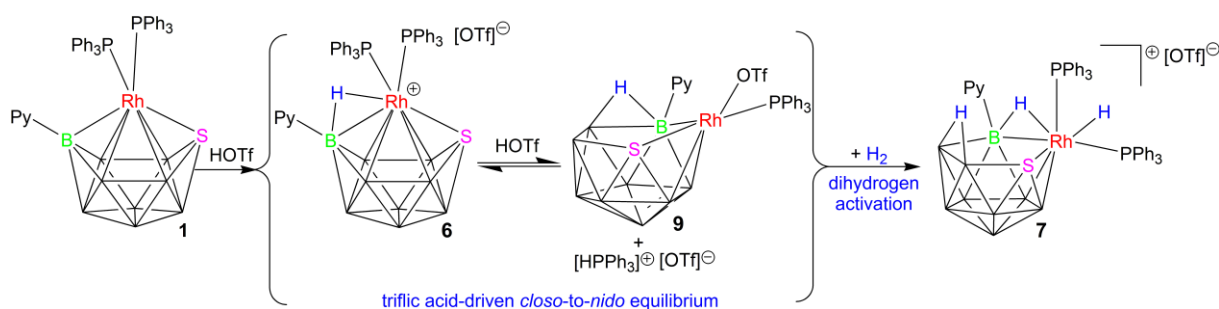
Beatriz Calvo, Ramón Macías,* Maria Jose Artigas, Fernando J. Lahoz,
and Luis A. Oro

Departamento de Química Inorgánica, Instituto de Síntesis Química y Catálisis
Homogénea-ISQCH, Universidad de Zaragoza-CSIC, C/Pedro Cerbuna 12,
50009 Zaragoza, Spain.

E-mail: rmacias@unizar.es

10 February 2013

GRAPHICAL ABSTRACT



The protonation of *closo*-rhodathioboranes affords unusual cationic clusters. The proton enhances the Lewis acidity, and induces a remarkable lability in these compounds. Protonation of **1** with triflic acid results in the formation of an equilibrium that involves cationic **6**, neutral OTf-ligated **9** and [HPPH₃]⁺. This ionic system efficiently splits H₂.

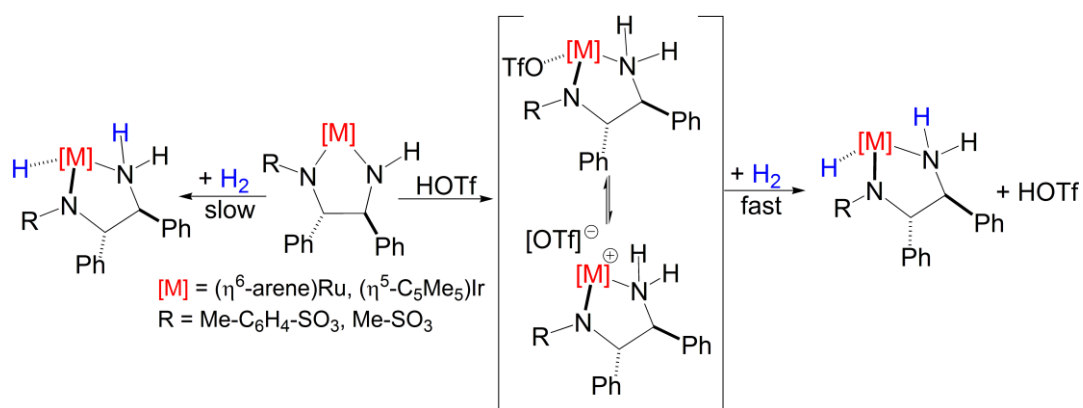
ABSTRACT

Treatment of [1,1-(PR₃)₂-3-(Py)-*closo*-1,2-RhSB₉H₈], where PR₃ = PMe₃ (**2**), or PPh₃ and PMe₃ (**3**), and Py = pyridine, with triflic acid (HOTf) affords [1,3-μ-(H)-1,1-(PR₃)₂-3-(Py)-1,2-RhSB₉H₈]⁺, where PR₃ = PMe₃ (**4**), or PMe₃ and PPh₃ (**5**). The products result from the protonation of the 11-vertex *closo*-cages at the Rh(1)-B(3) edge. These unusual cationic rhodathioboranes are stable in solution and in the solid state, and they have been fully characterized by multinuclear NMR spectroscopy. In addition, compound **5** has been characterised by single-crystal X-ray diffraction. A remarkable feature in this analysis is the presence of three {Rh(PPh₃)(PMe₃)}-to-{ηⁿ-SB₉H₈(Py)} (n = 4 or 5) conformers in the unit cell, giving an uncommon case of conformational isomerism. [1,1-(PPh₃)₂-3-(Py)-*closo*-1,2-RhSB₉H₈] (**1**), the *bis*-PPh₃-ligated analogue of **2** and **3**, is also protonated with HOTf, but, in marked contrast, the resulting cation [1,3-μ-(H)-1,1-(PPh₃)₂-3-(Py)-1,2-RhSB₉H₈]⁺ (**6**) is attacked by triflate anion with release of a PPh₃ ligand and formation of [8,8-(OTf)(PPh₃)-9-

(Py)-*nido*-8,7-RhSB₉H₉] (**9**). The result is an equilibrium that involves cationic species **6**, neutral OTf-ligated **9** and [HPPh₃]⁺, formed upon protonation of the released PPh₃ ligand. The resulting ionic system reacts readily with H₂ to give cationic [8,8,8-(H)(PPh₃)₂-9-(Py)-*nido*-8,7-RhSB₉H₉]⁺ (**7**). The reactivity is markedly higher than that previously found for **1**. And it introduces a new example of proton-assisted H₂ activation that occurs on a polyhedral boron-containing compound.

INTRODUCTION

Protonation of transition metal complexes is fundamental chemistry that induces an enhancement of the Lewis acidity of the metal centres,^[1] and it is relevant to many catalytic processes, including ionic hydrogenation and the reduction of H⁺ to H₂.^[2] Complexes that feature a metal/N-H bifunctional synergic effect are very efficient in the transfer of two atoms of hydrogen from organic molecules such as isopropanol and formic acid to polar C=E bonds (E = O or N).^[3] Among this important class of compounds, complexes (η⁶-arene)Ru[k²(N,N')TsNCHC₆H₅CHC₆H₅NH] (Ts = Me-C₆H₄-SO₃) and (η⁵-C₅Me₅)Ir[k²(N,N')MsNCHC₆H₅CHC₆H₅NH] (Ms = Me-SO₃) are of specific relevance to this paper. These complexes exhibit low reactivity toward H₂ under mild conditions,^[4] but treated with strong acids such as triflic they became good hydrogenation catalysts.^[5] The key is the generation of labile OTf-ligated complexes or salts, (η⁶-arene)Ru(OTf)[k²(N,N')TsNCHC₆H₅CH-C₆H₅NH₂] and (η⁵-C₅Me₅)Ir[k²(N,N')MsNCHC₆H₅CHC₆H₅-NH₂][OTf], which can accept the hydrogen molecule to form η²-H₂ species that lead to the heterolytic splitting of the H-H bond. Thus, the enhancement of the Lewis acidity, promoted by protonation, together with the formation of formally unsaturated complexes, lead to an efficient activation of H₂ (Scheme 1).

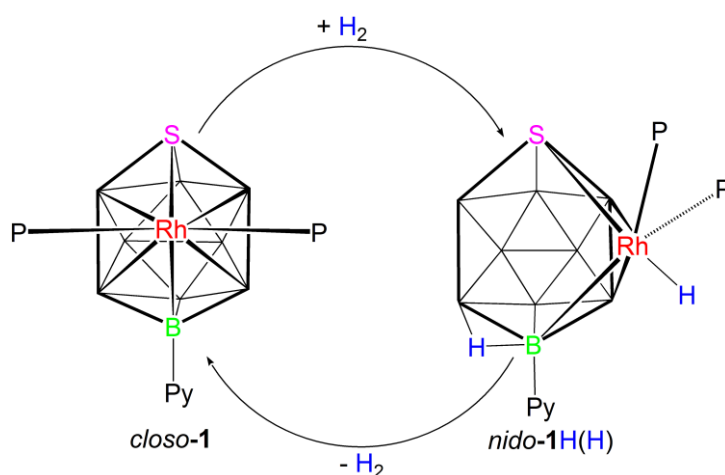


Scheme 1. Proton-assisted vs. non-assisted addition of hydrogen to diamido complexes

In the proton-assisted hydrogen activation by this type of metal amide complexes,^[6] the metal and the ligand simultaneously participate in the bond forming and breaking process. Complexes that combine the reactivity of the ligands and the metal centre are becoming important in synthesis, bond activation and catalysis.^[7] Many relevant examples involve the activation of an E-H bond at the transition element centre followed by proton transfer to the ligand backbone.^[8]

Classical *closo*→*nido* transformations in metallaboranes and metallaheteroboranes can be regarded as a type of metal-ligand cooperation that implies an oxidative / reductive flexibility in the clusters. The 11-vertex rhodathiaborane pair, [1,1-(PPh₃)₂-3-(Py)-*closo*-1,2-RhSB₉H₈] (**1**) and [8,8,8-(H)(PPh₃)₂-9-(Py)-*nido*-8,7-RhSB₉H₉] (**1H(H)**), where Py = pyridine, exhibits a remarkable *nido-to-closo* redox flexibility, leading to slow H₂ activation (Schemes 2 and 5).^[9] The result is the splitting of the H-H bond on the *closo*-cluster to give an Rh-H hydride ligand and a bridging B-H-B hydrogen atom to form the *nido* partner. This reaction is consistent with the thesis that the introduction of one electron pair into a *closo* cluster opens the cage.^[10] Recently, we have discovered that the rhodathiaborane **1** undergoes a *closo*→*nido* structural and electronic response to HCl, supporting the bifunctional character these 11-vertex rhodathiaboranes.^[11]

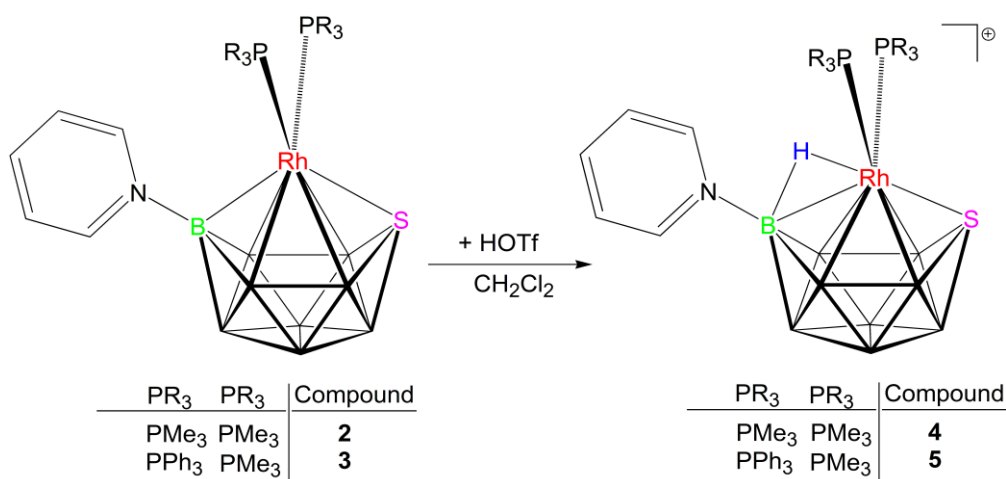
Herein, we report on the reactivity of 11-vertex *closo*-rhodathiaboranes with triflic acid, which affords unusual cationic clusters formed by simple protonation of the cages. In the case of the rhodathiaborane **1**, the protonation facilitates triflate attack on the cluster with release of PPh₃. The result is an equilibrium that involves a cationic *closo*-cluster and a neutral OTf-ligated *nido*-cage. This system reacts rapidly with H₂, and it may therefore be regarded as an acid-assisted hydrogen activation by polyhedral boron-containing compounds.



Scheme 2. Hydrogen mediated 11-vertex *closo*→*nido*→*closo* conversion.

RESULTS AND DISCUSSION

The reaction of [1,1-(PR₃)₂-3-(Py)-*closo*-1,2-RhSB₉H₈]^[12] where PR₃ = PMe₃ (**2**), or PPh₃ and PMe₃ (**3**), with triflic acid leads to protonation of the clusters and formation of polyhedral cations of formula [1,3-μ-(H)-1,1-(PR₃)₂-3-(Py)-1,2-RhSB₉H₈]⁺, where PR₃ = PMe₃ (**4**), or PMe₃ and PPh₃ (**5**).



Scheme 3. Protonation of 11-vertex rhodathiaboranes.

Characterized by spectroscopic means, these compounds maintain in solution the basic 11-vertex *closo*-structure of the neutral parent clusters (see supporting information, Figures S0-S21). Thus, the ^{11}B NMR spectrum of **4** exhibits six resonances in a 1:1:2:1:2:2 relative intensity ratio, which, with a slight overall deshielding, resembles readily the spectrum of **2** (Figure S1). Likewise, the ^{11}B NMR spectrum of the cationic analogue **5** shows a clear resemblance to **3** (Figure S2), revealing also a slight overall deshielding of the boron resonances in the protonated *versus* the neutral cluster. The $^{31}\text{P}\{-^1\text{H}\}$ NMR spectra of **4** and **5** support their C_s and C_1 point group symmetries, respectively. The former exhibits a doublet at δ -6.9 ($^1J(\text{Rh},\text{P}) = 99$ Hz), shifted around 3 ppm toward high frequency with respect the neutral **2** (Figure S3). The second cationic cluster shows two doublets of doublets at δ +33.9 ($^1J(\text{Rh},\text{P}) = 114$ Hz) and +6.3 ($^1J(\text{Rh},\text{P}) = 96$ Hz), which are safely assigned to the PPh₃ and PMe₃ ligands, respectively (Figure S4). It is noteworthy that the PMe₃ group suffers a high-frequency shift of the same order as that commented for the *bis*-PMe₃-ligated counterpart, **4**; in contrast, the PPh₃ resonance shifts toward low frequency when compared with **3**.

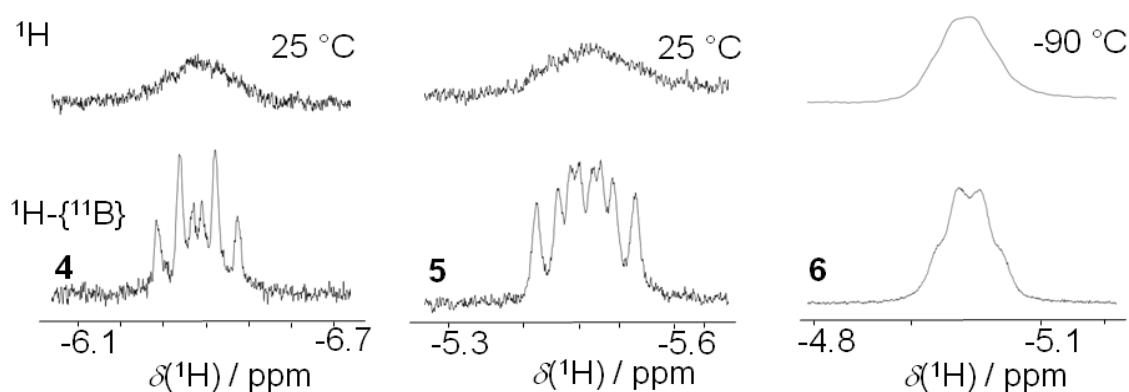


Figure 1. ^1H NMR resonances assigned to the Rh(1)-H-B(3) bridging hydrogen atom in **4-6**.

In the negative region of the $^1\text{H}\{-^{11}\text{B}\}$ NMR spectrum, **4** and **5** show multiplets that broaden when the boron broad-band decoupling is turned off (Figure 1). $^1\text{H}\{-^{11}\text{B}_{\text{sel}}\}$ experiments show that selective irradiation of the pyridine-substituted B(3) atom results in a sharpening of these broad resonances (Figure S0, page S3). This fact and the multiplicity of the peaks demonstrate that the protonation of the clusters takes place at the Rh(1)-B(3) edge, leading to the formation of a bridging Rh-H-B unit. Therefore, the resonances due to these bridging hydrogen atoms are diagnostic of the formation of the cationic clusters.

In both protonated clusters the $^1J(\text{Rh},\text{P})$ coupling constants decrease by around 46 Hz with respect to the neutral counterparts, suggesting that the new Rh(1)-H-B(3) bridging-bound hydrogen atom exerts a strong influence to the *exo*-polyhedral phosphine ligands, and, therefore, to the rhodium-to-thiaborane bonding interaction (*vide infra*).

A single crystal of **5** was analyzed by X-ray diffraction (Figure 2, Table 1). The compound crystallized in the triclinic system, revealing an uncommon case of conformational isomerism.^[13] Thus, the asymmetric unit contains three different conformers with a distinct rhodium-to-thiaborane connectivity, and three triflate anions. Conformers **5a** and **5b** exhibit two long Rh(1)-B(4) distances at 2.617(9) and 2.7171(11) Å typical of *isonido*-clusters that feature a $\{\text{Rh}(1)\text{S}(2)\text{B}(4)\text{B}(7)\}$ quadrilateral open face,^[14] whereas **5c** shows a

{Rh(1)S(2)B(3)B(4)B(7)} pentagonal face (Rh(1)–B(4) 3.5187(9) Å). Therefore, three cationic clusters are found in the unit cell along the structural coordinate from a deltahedral *closo*-octadecahedron

to

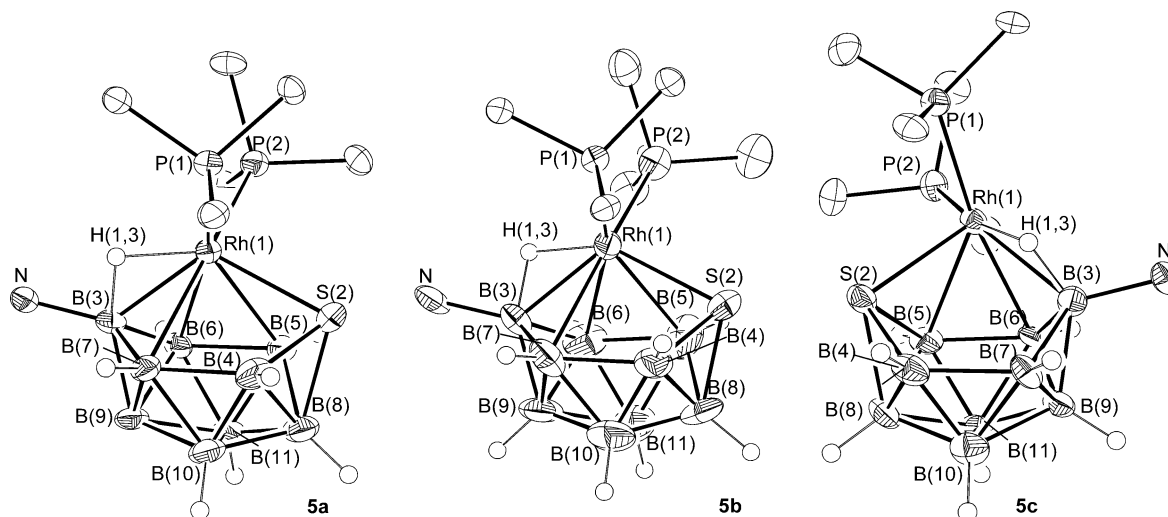


Figure 2. ORTEP-type of drawings of the three conformers found in the unit cell of **5** (closo-numbering scheme)

a *nido*-cage, suggesting that a change in the {Rh(H)(PPh₃)(PMe₃)}-to-{ηⁿ-SB₉H₈(Py)} coordination from *pentahapto* to *tetrahapto* requires very little energy. In other words, the proximity of metal-to-thiaborane conformational energies makes possible the existence of different isomers in the measured single-crystal of **5**.

Table 1. Selected lengths [Å] and angles [°] of isomers **5a**, **5b** and **5c**.^[a]

	5a	5b	5c
Rh(1)–S(2)	2.3786(19)	2.364(2)	2.4383(18)
Rh(1)–P(1)	2.3544(18)	2.335(2)	2.3419(19)
Rh(1)–P(2)	2.321(2)	2.331(2)	2.2798(19)
Rh(1)–B(3)	2.080(8)	2.108(8)	2.366(8)
Rh(1)–B(4)	2.617(9)	2.7171(11)	3.5187(9)

Rh(1)–B(5)	2.473(8)	2.426(11)	2.273(8)
Rh(1)–B(6)	2.368(7)	2.357(9)	2.247(8)
Rh(1)–B(7)	2.458(8)	2.496(9)	3.571(8)
P(1)–Rh(1)–P(2)	96.62(7)	98.00(8)	97.14(7)
P(1)–Rh(1)–S(2)	99.18(7)	99.30(8)	93.17(6)
P(2)–Rh(1)–S(2)	97.40(7)	98.82(8)	106.76(7)
P(1)–Rh(1)–B(3)	119.9(2)	115.8(3)	114.8(2)
P(2)–Rh(1)–B(3)	122.6(3)	126.3(2)	142.6(2)
B(3)–Rh(1)–S(2)	116.2(2)	114.1(3)	91.01(19)

[a] To facilitate comparison, the 11-vertex *closo*-numbering is used.

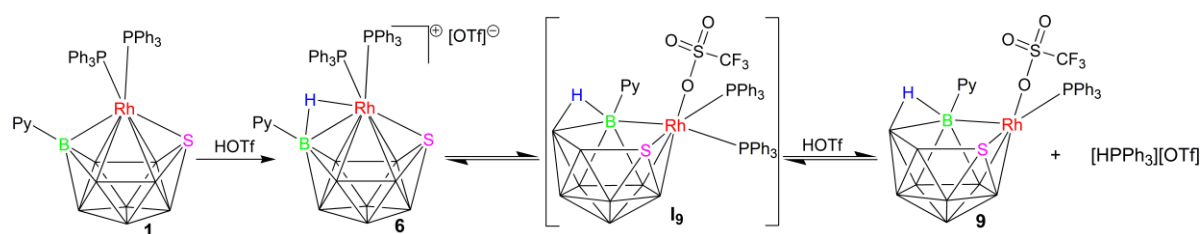
In the literature, there are numerous examples of protonation reactions of polyhedral boron-containing compounds, which have dealt with mainly anionic species that resulted in neutral products.^[15] As far as we are aware, the compounds **4**, **5** and **6** (*vide infra*), reported here, together with the recent published hydridorhodathiaborane [8,8,8-(H)(PPh₃)₂-9-(Py)-*nido*-8,7-RhSB₉H₁₀]⁺ (**7**, Scheme 5 below),^[11] represent the first examples of polyhedral cations formed by protonation of neutral boron-based clusters. The number of reported cationic boranes and metallaheteroboranes is small.^[16] The formers are represented mainly by small boron cages formed by heterolytic cleavage with Lewis bases; whereas cationic metallaheteroboranes (including the large subclass of metallacarboranes) generally contain charge-compensating ligands; and these are somewhat different in nature from the cations we describe in the present work.

In contrast to **2** and **3**,^[12] the *bis*-PPh₃-ligated analogue, **1**,^[9b] has a more complicated response to the treatment with triflic acid. Thus, no Rh(1)-H-B(3) bridging proton-resonance is observed after the addition of 0.5 equiv of HOTf in CD₂Cl₂ at room temperature (Figure S5); and the ³¹P-¹H NMR spectrum shows, in a 1:1:0.2 relative intensity ratio, the doublet of the

starting reagent **1** at $\delta +39.6$ ($^1J(\text{Rh},\text{P}) = 150$ Hz) together with a very broad peak in the range $\delta +34$ to $+26$, and a singlet at $\delta +3.0$; the latter attributable to the formation of $[\text{HPPH}_3]^+$ (Figure S6). Upon addition of another 0.5 equiv, the concentration of **1** decreases, whereas the intensity of the broad peak increases to show a broad doublet at $\delta +32.0$ ppm ($^1J_{\text{RhP}} \approx 151$ Hz), slightly overlapping a very broad signal between $\delta +34$ and $+26$ and the peak of $[\text{HPPH}_3]^+$ to give a 1:5:1 relative intensity pattern, respectively (Figure 3). After addition of another 0.5 equiv of HOTf, the $^{31}\text{P}\{-^1\text{H}\}$ resonance due to **1** disappears and the spectrum shows a doublet at $\delta +32.1$ ($^1J(\text{Rh},\text{P}) = 150$ Hz) and the singlet of $[\text{HPPH}_3]^+$ in a 1:1 ratio (Figure S8). With a total of 2.5 equiv of HOTf and at room temperature, the ratio of the doublet to the $[\text{HPPH}_3]^+$ singlet becomes 1:1.4 (Figure S10).

In the corresponding ^1H NMR spectra at ambient temperature, no hydride resonances were observed upon the consecutive additions of HOTf from 0.5 to 2.5 equiv (Figures S5, S12 to S14). However, the resonance of $[\text{HPPH}_3]^+$ cation at $\delta +9.08$ ($^1J(\text{P},\text{H}) = 530.4$ Hz) increases with the concentration of the acid.

Variable temperature (VT) NMR experiments provide valuable information dealing with the reactivity of **1** with triflic acid (Figures S5 to S14). Thus, the broad resonances in $^{31}\text{P}\{-^1\text{H}\}$ NMR spectra after addition of 0.5 (Figure S6) and 1.0 equiv (Figure 3) of HOTf become a sharp doublet at $\delta +32.2$ ($^1J_{\text{Rh-P}} = 105$ Hz) when the temperature is -50 °C or -90 °C. This resonance differs from that found in the room temperature $^{31}\text{P}\{-^1\text{H}\}$ NMR spectrum when the total addition of HOTf is 1.5 equiv ($\delta +32.0$, $^1J_{\text{Rh-P}} = 150$ Hz, Figure S8). At this point, a decrease in the temperature results in a 0.6 ppm shift to higher frequency for this doublet, and the appearance of a second doublet at $\delta +32.1$ ($^1J_{\text{Rh-P}} = 105$ Hz) which overlaps with the former (Figure S8). This second ^{31}P resonance resembles the doublet observed in the low temperature $^{31}\text{P}\{-^1\text{H}\}$ NMR spectra measured after the addition of a total of 0.5 and 1.0 equiv of acid (Figures S6 and S7).



Scheme 4. Proposed equilibria upon treatment of **1** with triflic acid.

These VT-NMR changes are reflected in the corresponding ¹H NMR spectra. Thus, with 0.5 and 1.5 equiv of HOTf the low temperature spectra show a hydride resonance at δ -5.03 which sharpens upon broadband boron decoupling (Figure S5 and S12). This fact, and the multiplicity of the peak (shown in Figure 1), are diagnostic of the formation of the cationic cluster, [1,3-μ-(H)-1,1-(PPh₃)₂-3-(Py)-1,2-RhSB₉H₈]⁺ (**6**), an analogue of compounds **4** and **5**. Interestingly, with 2.0 and 2.5 equiv of HOTf, the Rh(1)-H-B(3) proton resonance is not observed in the ¹H NMR spectra at room and low temperatures (Figures S13 and S14), and the ³¹P spectra resemble those found at room temperature upon addition of 0.5 to 1.5 equiv of HOTf (Figures S6-S8).

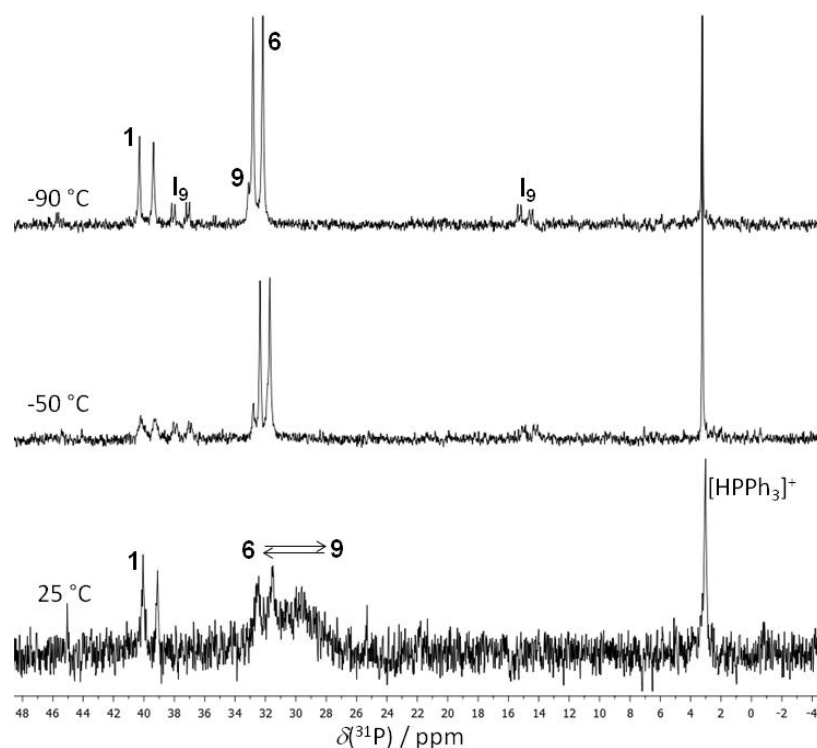
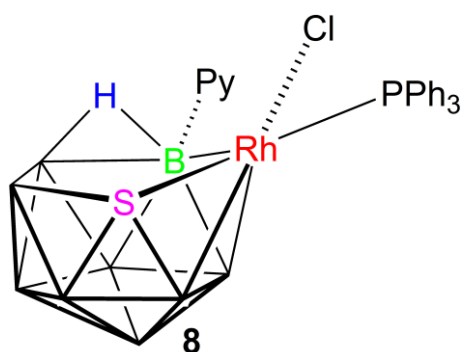


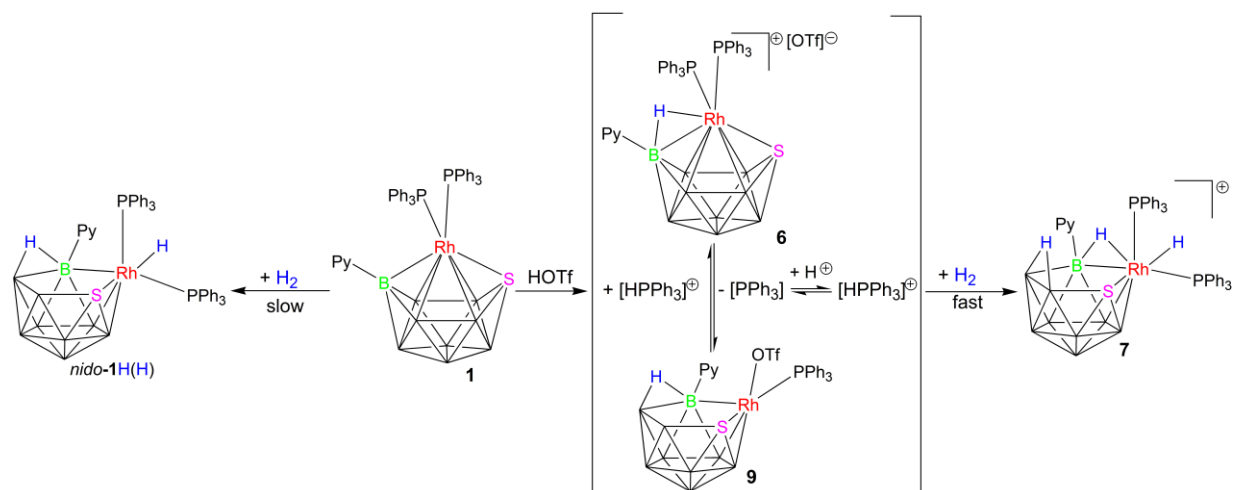
Figure 3. VT ³¹P-{¹H} NMR spectra of **1** after addition of 1 equiv of HOTf.

^{11}B NMR data at room temperature confirm further the changes that the *closo*-rhodathiaborane **1** suffers upon reaction with triflic acid. Thus, after addition of 0.5 equiv of HOTf the spectrum shows the appearance of new broad peaks in the range δ +20 to -30; addition of a total of 1 equiv results in the disappearance of the peaks corresponding to **1** and formation of a new spectrum that exhibits a 2:2:1:1:1:1 relative intensity ratio (Figure S15). Interestingly, consecutive addition of HOTf does not result in a significant change of the room temperature $^{11}\text{B}\{-^1\text{H}\}$ NMR spectrum, thus contrasting to the changes observed in the $^{31}\text{P}\{-^1\text{H}\}$ and ^1H NMR spectra. In any event, the new ^{11}B NMR spectra demonstrate that the *closo*-rhodathiaborane undergoes a significant cluster rearrangement. A comparison of these spectra with the $^{11}\text{B}\{-^1\text{H}\}$ NMR spectrum of crystallographically determined [8,8-(Cl)(PPh₃)-9-(Py)-*nido*-8,7-RhSB₉H₉] (**8**),^[11] reveals a close similarity which suggests that at ambient temperature, in the time scale of the NMR spectroscopy, the species present in solution after addition of triflic acid have an overall 11-vertex *nido*-structure. This resemblance is also apparent in the $^{31}\text{P}\{-^1\text{H}\}$ NMR spectrum, which for the Cl-derivative **8** shows a doublet at δ +32.2 with a $^1J(\text{Rh},\text{P})$ coupling constant of 153 Hz that compares readily to the room temperature spectrum that results after addition of more than 1.0 equiv of HOTf to **1**. Thus, according to this connexion, we postulate that the triflate-ligated species [8,8-(OTf)(PPh₃)-9-(Py)-*nido*-8,7-RhSB₉H₉] (**9**) is formed in this reaction. $^{19}\text{F}\{-^1\text{H}\}$ NMR data confirm the presence of coordinated triflate ligands. In particular, the $^{19}\text{F}\{-^1\text{H}\}$ NMR spectrum at room temperature of **1**, after addition of 0.5 equiv of HOTf, exhibits three low intensity triflate CF₃ singlets at δ -77.3, -77.4 and -78.1, and a high intensity peak at δ -78.8 (Figure S16). Upon cooling, the four peaks shift upfield. The high intensity resonance moves to δ -79.2 at -90 °C, approaching the value for free triflate ion, whereas the other three low intensity peaks remain below δ -78.7, suggesting the presence of coordinated triflate ligands. This is further supported by the low resolution mass spectrum of samples of **1** treated with 2.0 equiv of

HOTf, which gave a peak with an isotope pattern that matches well a compound of formulation $[(\text{OTf})_2\text{RhSB}_9\text{H}_7(\text{Py})]$.



These experimental data allow us to propose a reaction mechanism for the reaction of **1** with HOTf. At low concentrations of HOTf and at low temperatures, the *closo*-cluster undergoes protonation to give cation **6**, analogue of **4** and **5**. Compared to these cationic counterparts, **6** exhibits a remarkable lability in solution, which is demonstrated by the broadening in the $^{31}\text{P}\{-^1\text{H}\}$ NMR spectrum at room temperature and the disappearance of the



Scheme 5. Proton-assisted vs. non-assisted: two routes of hydrogen activation.

Rh(1)-H-B(3) hydride resonance in the $^1\text{H}\{-^{11}\text{B}\}$ spectrum. These results suggest a rapid proton exchange between **6** and the free acid. Additionally, the small amounts of $[\text{HPPH}_3]^+$ present in solution after the addition of 0.5 equiv of HOTf, and the appearance of new

resonances in the $^{11}\text{B}\{-^1\text{H}\}$ spectrum, suggest that there are other compounds involved in this equilibrium. Thus, the appearance of a second species is confirmed at higher concentrations of acid, and, according to the NMR data, this compound may be characterised as the OTf-ligated **9**. The formation of this compound is concomitant with the increase in the concentration of the triphenylphosphonium ion. This supports that the cation **6** is attacked by free triflate, leading to the release of PPh_3 that is then protonated to give $[\text{HPPH}_3]^+$. It could be postulated that the extrusion of PPh_3 ligand occurs from a *bis*- PPh_3 -ligated intermediate, $[\text{8,8,8-(OTf)(PPh}_3)_2\text{-9-(Py)-nido-8,7-RhSB}_9\text{H}_9]$ (**I₉**), which, as illustrated in Scheme 4, could be in equilibrium with **6**. In this regard, the low intensity doublets of doublets at $\delta +37.6$ and $+14.9$ in the $^{31}\text{P}\{-^1\text{H}\}$ NMR spectrum at $-50\text{ }^\circ\text{C}$ (Figure 3) could be ascribed to this intermediate. The fact that the room temperature $^{11}\text{B}\{-^1\text{H}\}$ NMR spectrum remains invariable at different acid concentrations (between 1.0 to 2.5 equiv), is a sign of rapid equilibria between all the species (Scheme 4).

The acid-induced opening of *closo*- $[(\text{PPh}_3)_2\text{RhSB}_9\text{H}_8(\text{Py})]$ (**1**) in triflic acid can be related to the cage-opening of $[\text{closo-B}_{10}\text{H}_{10}]^{2-}$ with strong acids that, in the presence of 2 equiv of ligand, produces *arachno*- $\text{B}_{10}\text{H}_{12}(\text{ligand})_2$, and, in the absence of ligand, apparently gives a high-energy borocation $[\text{B}_{10}\text{H}_{13}]^+$.^[17] The results reported here rein demonstrate that the proton-assisted opening is a stepwise process, which starts with the protonation of the *closo*-cage that induces an enhancement of the Lewis acidity of the system, facilitating the subsequent attack by nucleophiles. The resulting triflic acid-driven cationic *closo*- / neutral *nido*-cage, **6** / **9**, equilibrium has no precedent in polyhedral boron chemistry and, as far as we are aware, the substitution of a metal-bound PPh_3 ligand by a weakly coordinating triflate anion is not a typical reaction in the broader area of transition element complexes.

In CD_2Cl_2 at room temperature, the treatment of **1** with 0.5 equiv of HOTf and subsequent exposure to an H_2 atmosphere leads to the formation of the previously reported cationic 11-

vertex hydridorhodathiaborane **7**.^[11] Comparison of the $^{31}\text{P}\{-^1\text{H}\}$ and $^1\text{H}\{-^{11}\text{B}\}$ NMR spectra before and after the exposure to hydrogen (Figures S19 and S20), demonstrates that the reaction involves species **6**, **9** and the phosphonium ion of the proposed equilibrium (Scheme 3), which in minutes react with H_2 to give **7**, whereas the concentration of **1** remains virtually unchanged. The presence of a small amount of the neutral hydridorhodathiaborane, **1H(H)**, inferred from the low intensity of the ^1H resonances at δ -1.39 (BHB) and -12.46 (Rh-H), could be due to some hydrogenation of **1** (Scheme 2).

At higher concentrations of acid, the reaction with hydrogen is hindered, as demonstrated by the fact that the formation of **7** is not quantitative; as some $[\text{HPPH}_3]^+$ and **9** remains in solution (Figure S21). This suggests that the protonated cluster **6**, or some intermediates formed along the pathway of the **6** / **9** equilibrium are most likely responsible for the facile activation of H_2 . The conformational isomerism of the cationic cluster **5** and the equilibrium between **6** and **9**, indicate that $\{\text{Rh}(\text{PR}_3)_2\}$ -to- $\{\eta^n\text{-SB}_9\text{H}_8(\text{Py})\}$ conformational changes can be produced at a low energy cost in this system. It is, therefore, possible to postulate that the interaction between the hydrogen molecule and the cationic species is facilitated by the intrinsic lability of the system, resulting in the heterolytic splitting of the H-H bond. Treatment of **1** with HCl merely affords the Cl-ligated derivative **8**, which does not react with H_2 —most probably due to the strong coordination of chlorine anion.^[11]

CONCLUSION

Triflic acid protonates the 11-vertex rhodathiaboranes **1**, **2** and **3** to afford unusual polyhedral cations. The proton enhances the Lewis acidity of the clusters, resulting in a higher reactivity. In this regard, the three conformers found in a crystal of compound **5** indicate that the metal-to-thiaborane linkage is non-rigid and that conformational changes can be produced at a low energy cost in this system. More remarkable is the proton-induced lability of compound **1**,

which yields a cationic rhodathiaborane that reacts with triflate anion, and undergoes PPh₃ ligand substitution to afford the neutral OTf-ligated compound **9**. The resulting system is in equilibrium, and it reacts readily with H₂. The combined enhancement of Lewis acidity and conformational lability favour the interaction of hydrogen with the cages, leading to the splitting of H₂. Addition of H₂ to a metallaheteroborane has been reported only once before.^[9a] This reaction involves the PPh₃-ligated *closo*-cluster **1** which reacts only slowly with H₂.^[9] This work, therefore, represents a significant case of proton-assisted hydrogen activation via metal-thiaborane cooperation by *closo-nido* cluster transformations.

These cationic rhodathiaboranes represent a potentially rich source of polyhedral Lewis acids.

EXPERIMENTAL SECTION

General Considerations: All reactions were carried out under an argon atmosphere using standard Schlenk-line techniques. Solvents were obtained from an Innovative Technology Solvent Purification System. All commercial reagents were used as received without further purification. The rhodathiaboranes [1,1-(PR₃)₂-3-(Py)-*closo*-1,2-RhSB₉H₈], where Py = Pyridine, PR₃ = PPh₃ (**1**), PMe₃ (**2**), or PPh₃ and PMe₃ (**3**) were prepared by published methods.^[9, 12] NMR spectra were recorded on Bruker Avance 300-MHz and AV 400-MHz spectrometers, using ¹¹B, ¹¹B-{¹H}, ¹H, ¹H{¹¹B}, ¹H{¹¹B(selective)} and ³¹P-{¹H} techniques. ¹H chemical shifts were measured relative to partially deuterated solvent peaks but are reported in ppm relative to tetramethylsilane. ¹¹B chemical shifts were measured relative to [BF₃(OEt)₂]. ³¹P (121.48 MHz) chemical shifts were measured relative to H₃PO₄ (85%). Mass spectrometry data were recorded on a VG Autospec double focusing mass spectrometer, on a microflex MALDI-TOF, and on a ESQUIRE 3000+ API-TRAP, operating in either positive or negative modes. In each case there was an excellent correspondence between the

calculated and measured isotopomer envelopes. A well-matched isotope pattern may be taken as a good criterion of identity.^[18]

X-ray structure analysis for compound 5: Crystals were grown by slow diffusion of hexane into a dichloromethane solution of **5**. A suitable crystal was coated with perfluoropolyether, mounted on a glass fiber and fixed in a cold nitrogen stream ($T = 100(2)$ K) to the goniometer head. Data collection were performed on a Bruker Kappa APEX DUO CCD area detector diffractometer with monochromatic radiation $\lambda(\text{MoK}\alpha) = 0.7107073 \text{ \AA}$, using narrow frames (0.3° in ω). The data were reduced (SAINT)^[19] and corrected for absorption effects by multiscan methods (SADABS).^[20] The structure was solved using the SHELXS-86 program,^[21] and refined against all F² data by full-matrix least-squares techniques (SHELXL-97).^[22] All non-hydrogen atoms were refined with anisotropic displacement parameters. Hydrogen atoms were included in calculated positions and refined with a positional and thermal riding model. The Rh(1)-H-B(3) bridging hydrogen atoms were not observed in the X-ray analysis but were predicted by potential-energy analysis calculations using the HYDEX program.^[23]

CCDC-907304 contains the supplementary crystallography data for this paper. These data can be obtained free of charge from the Cambridge Crystallographic Data Centre via [www.ccdc.cam.ac.uk/data request/cif](http://www.ccdc.cam.ac.uk/data_request/cif)

[1,3- μ -(H)-1,1-(PMe₃)₂-3-(Py)-*closo*-1,2-RhSB₉H₈][OTf] (4):

Low reaction scale: 7 mg of **2** (0.015 mmol) was dissolved in 0.3 mL of CD₂Cl₂ in a screw cap NMR tube, and then 1.31 μ L (0.015 mmol) of HOTf was added to the bright-yellow solution of the rhodathiaborane. The sample was examined by NMR spectroscopy at room temperature. The data revealed the quantitative formation of [1,1-(PMe₃)₂-3-(Py)-*closo*-1,2-RhSB₉H₉][OTf] (**4**). ¹¹B-{¹H} NMR (128 MHz; CD₂Cl₂; 298 K): δ 58.3 (1B, s, B-Py), 29.7 (1B, br, BH), 9.0 (1B, br, BH), -13.2 (1B, br, BH), -23.6 (2B, br, BH), -24.9 (1B, br, BH). ¹H-

{¹¹B} NMR (400 MHz, CD₂Cl₂, 300 K): δ +9.20 (2H, d, ²J(H,H) = 4.3 Hz, *H_o*-Py), +8.50 (1H, t, *H_p*-Py), +8.07 (2H, t, *H_m*-Py), +4.70 (1H, s, BH), +2.87 (1H, s, BH), +1.58 (18H, d, ²J(P,H) = 8.6 Hz, PMe₃), +1.46 (1H, s, BH), +0.75 (1H, s, BH), +0.40 (1H, s, BH), -6.70 (1H, dt, ¹J(Rh,H) = 25 Hz, ²J(P,H) = 16 Hz, B-H-Rh). ³¹P-{¹H} NMR (162 MHz; CD₂Cl₂; 298 K): δ -6.7 (d, ¹J(P,Rh) = 99 Hz). ¹⁹F-{¹H} NMR (282 MHz, CD₂Cl₂, 300 K): δ -78.9 (OTf). LRMS (MALDI⁺, DIT): *m/z* calcd for B₉C₁₁H₃₂NP₂RhS⁺: 473 [M]⁺; found: 473, isotope envelope that matches that calculated from the known isotopic abundances of the constituent elements.

Higher reaction scale: 30 mg of **2** (0.0636 mmol) was dissolved in 7 mL of CH₂Cl₂ in a Schlenk tube. To the resulting orange-red solution, 5.6 mL (9.547 mg, 0.0636 mmol) of triflic acid was added with a microsyringe. The reaction mixture was stirred for 15 minute under an atmosphere of argon. After this time, the solvent was reduced in volume under *vacuum* and hexane was added to obtain a red oily product that was separated and characterized as **4**. Yield: 28 mg (0.044 mmol, 70 %).

[1,3-μ-(H)-1,1-(PMe₃)(PPh₃)-3-(Py)-closo-1,2-RhSB₉H₉][OTf] (5): 4.2 mg of **3** (0.0064 mmol) was dissolved in 0.3 mL of CD₂Cl₂ in a screw cap NMR tube, and then 0.57 μL (0.0064 mmol) of HOTf was added to the bright-yellow solution of the rhodathiaborane. The reaction mixture was examined by NMR spectroscopy at room temperature. The data revealed the quantitative formation of **5**. ¹¹B-{¹H} NMR (128 MHz; CD₂Cl₂; 298 K): δ +57.8 (1B, s, B-Py), +29.6 (1B, br, BH), +9.0 (1B, br, BH), -21.8 (1B, br, BH), -23.6 (2B, br, BH), -26.2 (1B, br, BH). ¹H-{¹¹B} NMR (400 MHz, CD₂Cl₂, 300 K): δ +9.13 (2H, d, ²J(H,H) = 5.5 Hz, *H_o*-Py), +8.50 (1H, t, *H_p*-Py), +7.02 (2H, t, *H_m*-Py), +7.6-7.3 (15H, m, PPh₃), +4.64 (1H, s, BH), +2.87 (1H, s, BH), +1.28 (3H, d, ²J(P,H) = 11.2 Hz, PMe₃), +0.70 (1H, s, BH), +0.58 (1H, s, BH), +0.42 (1H, s, BH), -0.14 (1H, s, BH), -5.48 (1H, ddd, ¹J(Rh,H) = 24 Hz, ²J(P,H) = 12 Hz, ²J(P,H) = 11 Hz, B-H-Rh). ³¹P-{¹H} NMR (162 MHz; CD₂Cl₂; 298 K): δ +36.2 (1P, dd, ¹J(P,Rh) = 114 Hz, ²J(P,P) = 22 Hz, PPh₃), -7.3 (1P, dd, ¹J(P,Rh) = 96 Hz, ²J(P,P) = 22 Hz, PMe₃). ¹⁹F-{¹H} NMR (282 MHz, CD₂Cl₂, 300 K): δ -78.8 (OTf). LRMS

(MALDI⁺/DIT): m/z calcd for B₉C₂₆H₃₈NP₂RhS : 659 [M]⁺; found 659, isotope envelope matching that calculated from the known isotopic abundances of the constituent elements.

Reaction of [1,1-(PPh₃)₂-3-(Py)-closo-1,2-RhSB₉H₈] (1) with HOTf: 8.4 mg of 3 (0.01 mmol) was dissolved in 0.3 mL of CD₂Cl₂ in a screw cap NMR tube, and then 0.44 μL (0.005 mmol) of HOTf was added to the pale-yellow solution of the rhodathiaborane. Due to the lability of this system compounds [1,3-μ-(H)-1,1-(PPh₃)₂-3-(Py)-1,2-RhSB₉H₈]⁺ (**6**) and [8,8-(OTf)(PPh₃)-9-(Py)-nido-8,7-RhSB₉H₉] (**9**) were characterized *in situ* by NMR spectroscopy at different temperatures. ¹H-¹¹B NMR (500 MHz, CD₂Cl₂, 183 K): δ +8.79 to +8.15 (pyridinic signals), 7.65 to +6.85 (phenylic signals), +4.65 (br, BH), +4.44 (br, BH), +3.15 (br, BH), +2.46 (br, BH), +2.18 (br, BH), +1.88 (br, BH), +1.58 (br, BH), +1.39 (br, BH), +0.96 (br, BH), +0.47 (br, BH), -0.13 (br, BH), -0.31 (br, BH), -0.44 (br, BH), -5.03 (br. q, ¹J(Rh,H) + ²J(P,H) ≈ 16 Hz. ³¹P-¹H NMR (162 MHz; CD₂Cl₂; 183 K): δ +39.8 (d, ¹J(P,Rh) = 150 Hz, compound **1**), +37.6 (dd, ¹J(P,Rh) = 153 Hz, ²J(P,P) = 34 Hz, minor component proposed as intermediate **I**₉), +32.5 (d, ¹J(P,Rh) = 105 Hz, compound **6**), +14.9 (dd, ¹J(P,Rh) = 130 Hz, ²J(P,P) = 35 Hz, minor component proposed as intermediate **I**₉), +3.0 (s, [HPPPh₃]⁺). Data with a total of 1.5 equiv of HOTf (0.015 mmol, 1.33 μL), the resulting NMR data are: ¹H NMR (500 MHz, CD₂Cl₂, 183 K): δ +9.08 (d, ¹J(H,P) = 530.4 Hz, [HPPPh₃]⁺), +9.17 (Py), +8.75 (Py), +8.63 (Py), +8.10 (Py), +7.79 to +6.69 (phenylic signals), +4.33 (br, BH), +3.12 (br, BH), +2.16 (br, BH), +1.86 (br, BH), +0.94 (br, BH), -0.19 (br, BH), -5.01 (br m, Rh-H-B). ³¹P-¹H NMR (162 MHz; CD₂Cl₂; 183 K): δ +32.5 (d, ¹J(P,Rh) = 149 Hz, PPh₃, **9**), +32.2 (d, ¹J(P,Rh) = 105 Hz, PPh₃, **6**), +3.6 (s, [HPPPh₃]⁺). LRMS (MALDI⁺, DIT): m/z calcd for C₁₆F₃S₂O₃Rh₁B₉H₂₄P₁: 617 [M-(NC₅H₅)]⁺; found 617, isotope envelope matching that calculated from the known isotopic abundances of the constituent elements.

Data with a total of 2.0 equiv of HOTf (0.02 mmol, 1.7 μL): ¹H NMR (500 MHz, CD₂Cl₂, 183 K): δ +8.89 (d, ¹J(H,P) = 526.8 Hz, [HPPPh₃]⁺), +9.16 (Py), +7.95 (Py), +7.79 to +6.90 (phenylic signals), +4.34 (br, BH), +3.43 (br, BH), +3.14 (br, BH), +1.60 (br, BH), +1.36 (br,

BH), +0.96 (br, BH). $^{11}\text{B}\{-^1\text{H}\}$ NMR (128 MHz; CD_2Cl_2 ; 298): δ +16.5 (1B, s, B-Py), +3.7 (2B, br, BH), -2.8 (1B, br, BH), -12.1 (2B, br, BH), -20.9 (1B, br, BH), -22.7 (1B, br, BH), -29.7 (1B, br, BH). $^{31}\text{P}\{-^1\text{H}\}$ NMR (162 MHz; CD_2Cl_2 ; 183 K): δ +32.8 (d, $^1J(\text{P,Rh}) = 148$ Hz, PPh_3 , 9), +4.9 (s, $[\text{HPPh}_3]^+$). LRMS (MALDI/DCTB): m/z 617 isotope envelop that corresponds to a molecular ion of formulation, $[(\text{OTf})_2(\text{Py})\text{RhSB}_9\text{H}_7]^-$.

Reactions with H_2 . *Experiment A:* 4.3 mg (0.005 mmol) of **1** was dissolved in 0.3 mL of CD_2Cl_2 in a quick pressure valve NMR tube, and then 0.22 μL (0.0025 mmol, 0.5 equiv) of HOTf was added. The sample was examined by NMR spectroscopy at room temperature, showing the formation of the equilibrium between **6**, **9** and $[\text{HPPh}_3]^+$, as well as the starting neutral cluster **1** (see Figure S19). The tube was evacuated under vacuum at the temperature of liquid nitrogen, and subsequently, exposed to 10 bar of hydrogen. The NMR spectra showed that **6**, **9** and $[\text{HPPh}_3]^+$ reacted with hydrogen to give compound **7**. Small amounts of **1** are also observed in the $^1\text{H}\{-^{11}\text{B}\}$ NMR spectrum (see Figure S20). *Experiment B:* 3.4 mg (0.004 mmol,) of **1** was dissolved in 0.3 mL of CD_2Cl_2 in a quick pressure valve NMR tube, and then 0.43 μL (0.0048 mmol, 1.2 equiv) of HOTf was added. The procedure was as described in experiment A for with 0.5 equiv of HOTf. The NMR data showed formation of **7** but with significant amounts of **6** and $[\text{HPPh}_3]^+$ in solution after the exposure of the sample to H_2 .

ACKNOWLEDGEMENTS

We acknowledge the Spanish Ministry of Science and Innovation (CTQ2009-10132, CONSOLIDER INGENIO, CSD2009-00050, MULTICAT and CSD2006-0015, Crystallization Factory) for support of this work. B.C. thanks the “Diputación General de Aragón” for a pre-doctoral scholarship.

RERERENCES

- [1] a) G. J. Kubas, in *Modern Inorganic Chemistry*, Kluwer Academic/Plenum, New York, **2001**; b) E. T. Papish, M. P. Magee, J. R. Norton, in *Recent Advances in Hydride Chemistry* (Eds.: M. Peruzzini, R. Poli), Elsevier, London, **2001**, pp. 39-74.
- [2] a) S. Michaile, M. Hillman, J. J. Eisch, *Organometallics* **1988**, *7*, 1059-1065; b) J. P. Collman, P. S. Wagenknecht, J. E. Hutchison, *Angew. Chem., Int. Ed. Engl.* **1994**, *33*, 1537-1554; c) G. J. Kubas, *Chem. Rev.* **2007**, *107*, 4152-4205; d) J. Rosenthal, D. G. Nocera, *Acc. Chem. Res.* **2007**, *40*, 543-553; e) M. H. V. Huynh, T. J. Meyer, *Chem. Rev.* **2007**, *107*, 5004-5064; f) R. M. Bullock, *Chem. Eur. J.* **2004**, *10*, 2366-2374; g) M. Martín, E. Sola, S. Tejero, J. A. López, L. A. Oro, *Chem. Eur. J.* **2006**, *12*, 4057-4068.
- [3] a) R. Noyori, S. Hashiguchi, *Acc. Chem. Res.* **1997**, *30*, 97-102; b) T. Ikariya, K. Murata, R. Noyori, *Org. Biomol. Chem.* **2006**, *4*, 393-406; c) T. Ikariya, A. J. Blacker, *Acc. Chem. Res.* **2007**, *40*, 1300-1308.
- [4] a) V. Rautenstrauch, X. Hoang-Cong, R. Churlaud, K. Abdur-Rashid, R. H. Morris, *Chem. Eur. J.* **2003**, *9*, 4954-4967; b) K.-J. Haack, S. Hashiguchi, A. Fujii, T. Ikariya, R. Noyori, *Angew. Chem., Int. Ed. Engl.* **1997**, *36*, 285-288; c) M. Ito, M. Hirakawa, K. Murata, T. Ikariya, *Organometallics* **2001**, *20*, 379-381.
- [5] a) C. A. Sandoval, T. Ohkuma, N. Utsumi, K. Tsutsumi, K. Murata, R. Noyori, *Chem. Asian. J.* **2006**, *1*, 102-110; b) T. Ohkuma, K. Tsutsumi, N. Utsumi, N. Arai, R. Noyori, K. Murata, *Org. Lett.* **2007**, *9*, 255-257; c) T. Ohkuma, N. Utsumi, M. Watanabe, K. Tsutsumi, N. Arai, K. Murata, *Org. Lett.* **2007**, *9*, 2565-2567; d) T. Ohkuma, N. Utsumi, K. Tsutsumi, K. Murata, C. Sandoval, R. Noyori, *J. Am. Chem. Soc.* **2006**, *128*, 8724-8725; e) S. Arita, T. Koike, Y. Kayaki, T. Ikariya, *Organometallics* **2008**, *27*, 2795-2802; f) C. A. Sandoval, Y. Li, K. Ding, R. Noyori, *Chem. Asian. J.* **2008**, *3*, 1801-1810.

- [6] a) Z. M. Heiden, T. B. Rauchfuss, *J. Am. Chem. Soc.* **2009**, *131*, 3593-3600; b) Z. M. Heiden, T. B. Rauchfuss, *J. Am. Chem. Soc.* **2006**, *128*, 13048-13049; c) Z. M. Heiden, B. J. Gorecki, T. B. Rauchfuss, *Organometallics* **2008**, *27*, 1542-1549.
- [7] J. I. van der Vlugt, J. N. H. Reek, *Angew. Chem., Int. Ed.* **2009**, *48*, 8832-8846.
- [8] C. Gunanathan, D. Milstein, *Acc. Chem. Res.* **2011**, *44*, 588-602.
- [9] a) A. Alvarez, R. Macias, M. J. Fabra, F. J. Lahoz, L. A. Oro, *J. Am. Chem. Soc.* **2008**, *130*, 2148-2149; b) A. Alvarez, R. Macias, J. Bould, M. J. Fabra, F. J. Lahoz, L. A. Oro, *J. Am. Chem. Soc.* **2008**, *130*, 11455-11466.
- [10] K. Wade, *Adv. Inorg. Chem. Radiochem.* **1976**, *18*, 1-66.
- [11] B. Calvo, R. Macías, C. Cunchillos, F. J. Lahoz, L. A. Oro, *Organometallics* **2012**, *31*, 2526-2529.
- [12] B. Calvo, Á. Álvarez, R. Macías, P. García-Orduña, F. J. Lahoz, L. A. Oro, *Organometallics* **2012**, *31*, 2986-2995.
- [13] J. Bernstein, *Polymorphism in Molecular Crystals*, Oxford University Press, Oxford, **2002**.
- [14] a) K. Nestor, X. L. R. Fontaine, N. N. Greenwood, J. D. Kennedy, J. Plešek, B. Štíbr, M. Thornton-Pett, *Inorg. Chem.* **1989**, *28*, 2219-2221; b) J. Bould, C. Cunchillos, F. J. Lahoz, L. A. Oro, J. D. Kennedy, R. Macías, *Inorg. Chem.* **2010**, *49*, 7353-7361.
- [15] a) D. M. Speckman, C. B. Knobler, M. F. Hawthorne, *Organometallics* **1985**, *4*, 426-428; b) B. E. Hodson, T. D. McGrath, F. G. A. Stone, *Organometallics* **2005**, *24*, 1638-1646; c) R. N. Grimes, J. R. Pipal, E. Sinn, *J. Am. Chem. Soc.* **1979**, *101*, 4172-4180; d) I. T. Chizhevskii, T. V. Zinevich, P. V. Petrovskii, V. I. Bregadze, *Metalloorg. Khim.* **1992**, *5*, 1088-1093; e) N. Carr, D. F. Mullica, E. L. Sappenfield, F. G. A. Stone, *Inorg. Chem.* **1994**, *33*, 1666-1673.

- [16] a) J. J. Solomon, R. F. Porter, *J. Am. Chem. Soc.* **1972**, *94*, 1443-1450; b) E. L. Muetterties, *Pure Appl. Chem.* **1965**, *10*, 53; c) P. Brint, E. F. Healy, T. R. Spalding, T. Whelan, *J. Chem. Soc., Dalton Trans.* **1981**, 2515-2522; d) E. J. M. Hamilton, H. T. Leung, R. G. Kultyshev, X. Chen, E. A. Meyers, S. G. Shore, *Inorg. Chem.* **2012**, *51*, 2374-2380; e) A. R. Kudinov, P. Zanello, R. H. Herber, D. A. Loginov, M. M. Vinogradov, A. V. Vologzhanina, Z. A. Starikova, M. Corsini, G. Giorgi, I. Nowik, *Organometallics* **2010**, *29*, 2260-2271; f) G. Ferguson, J. Pollock, P. A. McEneaney, D. P. Oconnell, T. R. Spalding, J. F. Gallagher, R. Macías, J. D. Kennedy, *Chem. Commun.* **1996**, 679-681; g) D. D. J. Ellis, Paul A.; Stone, F. Gordon A., *J. Chem. Soc., Dalton Trans.* **2000**, 2113, 2122; h) M. Kameda, M. Shimoi, G. Kodama, *Inorg. Chem.* **1984**, *23*, 3705-3709; i) M. Kameda, G. Kodama, *Inorg. Chem.* **1985**, *24*, 2712-2714; j) M. Kameda, G. Kodama, *J. Am. Chem. Soc.* **1980**, *102*, 3647-3649; k) R. Núñez, O. Tutusaus, F. Teixidor, C. Viñas, R. Sillanpää, R. Kivekäs, *Chem. Eur. J.* **2005**, *11*, 5637-5647; l) J. G. Planas, C. Viñas, F. Teixidor, M. E. Light, M. B. Hursthouse, H. R. Ogilvie, *Eur. J. Inorg. Chem.* **2005**, *2005*, 4193-4205; m) J. P. Sheehan, T. R. Spalding, G. Ferguson, J. F. Gallagher, B. Kaitner, J. D. Kennedy, *J. Chem. Soc., Dalton Trans.* **1993**, 35-42.
- [17] a) O. Bondarev, Y. V. Sevryugina, S. S. Jalisatgi, M. F. Hawthorne, *Inorg. Chem.* **2012**, *51*, 9935-9942; b) M. D. Marshall, R. M. Hunt, G. T. Hefferan, R. M. Adams, J. M. Makhlouf, *J. Am. Chem. Soc.* **1967**, *89*, 3361-3362.
- [18] W. Henderson, J. S. McIndoe, *Mass Spectrometry of Inorganic and Organometallic Compounds: Tools Techniques Tips*, John Wiley & Sons, **2005**.
- [19] Z. Otwinowski, W. Minor, in *Methods Enzymol.*, Vol. 276 (Ed.: J. R. M. S. C. W. Carter), Academic Press, New York, **1997**, pp. 307-326.
- [20] R. H. Blessing, *Acta Cryst.* **1995**, *A51*, 33.

[21]G. M. Sheldrick, University of Göttingen: Göttingen, Germany, **1997**.

[22]G. M. Sheldrick, *Acta Cryst.* **2008**, *A64*, 112-122.

[23]A. G. Orpen, *J. Chem. Soc., Dalton Trans.* **1980**, 2509-2516.